

## Synthesis of Bromoundecyl Resorc[4]arenes and Applications of the Cone Stereoisomer as Selector for Liquid Chromatography

Silvia Corradi, Giulia Mazzocanti, Francesca Ghirga, Deborah Quaglio, Laura Nevola, Chiara Massera, Franco Ugozzoli, Giuseppe Giannini, Alessia Ciogli, and Ilaria D'Acquarica

*J. Org. Chem.*, **Just Accepted Manuscript** • Publication Date (Web): 29 May 2018

Downloaded from <http://pubs.acs.org> on May 29, 2018

### Just Accepted

"Just Accepted" manuscripts have been peer-reviewed and accepted for publication. They are posted online prior to technical editing, formatting for publication and author proofing. The American Chemical Society provides "Just Accepted" as a service to the research community to expedite the dissemination of scientific material as soon as possible after acceptance. "Just Accepted" manuscripts appear in full in PDF format accompanied by an HTML abstract. "Just Accepted" manuscripts have been fully peer reviewed, but should not be considered the official version of record. They are citable by the Digital Object Identifier (DOI®). "Just Accepted" is an optional service offered to authors. Therefore, the "Just Accepted" Web site may not include all articles that will be published in the journal. After a manuscript is technically edited and formatted, it will be removed from the "Just Accepted" Web site and published as an ASAP article. Note that technical editing may introduce minor changes to the manuscript text and/or graphics which could affect content, and all legal disclaimers and ethical guidelines that apply to the journal pertain. ACS cannot be held responsible for errors or consequences arising from the use of information contained in these "Just Accepted" manuscripts.



# Synthesis of Bromoundecyl Resorc[4]arenes and Applications of the *Cone* Stereoisomer as Selector for Liquid Chromatography

Silvia Corradi,<sup>§</sup> Giulia Mazzocanti,<sup>§</sup> Francesca Ghirga,<sup>†</sup> Deborah Quaglio,<sup>§</sup> Laura Nevola,<sup>§,‡</sup> Chiara Massera,<sup>§§</sup> Franco Ugozzoli,<sup>††</sup> Giuseppe Giannini,<sup>‡‡</sup> Alessia Ciogli,<sup>§,\*</sup> and Ilaria D'Acquarica<sup>§,\*</sup>

<sup>§</sup> Dipartimento di Chimica e Tecnologie del Farmaco, Sapienza Università di Roma, P.le A. Moro 5, 00185 Roma, Italy.

<sup>†</sup> Center For Life Nano Science@Sapienza, Istituto Italiano di Tecnologia, Viale Regina Elena 291, 00161 Roma, Italy.

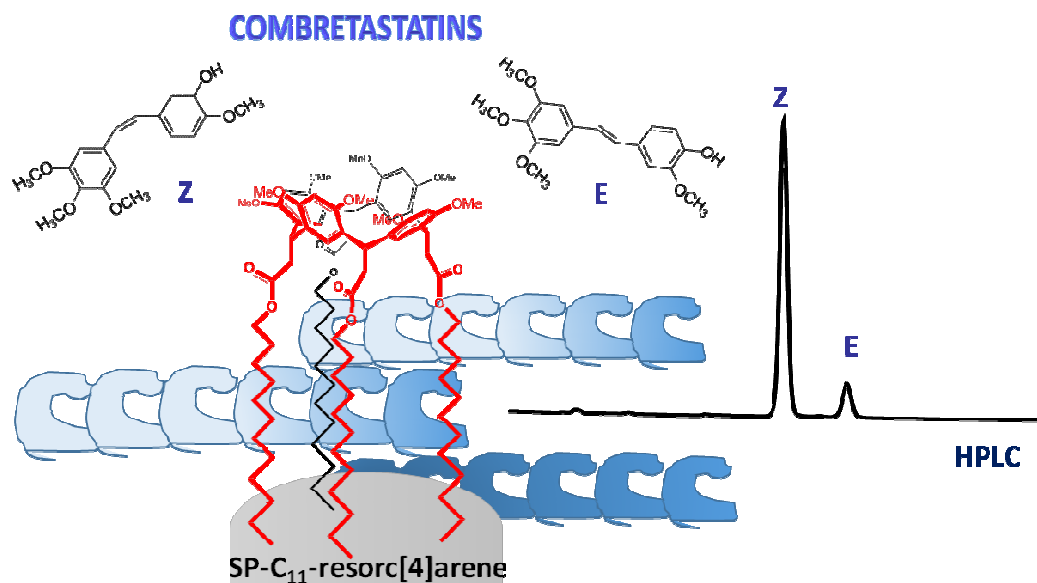
<sup>‡</sup> Institut de Recerca Biomèdica (IRB-PCB), Barcelona, Spain.

<sup>§§</sup> Dipartimento di Scienze Chimiche, della Vita e della Sostenibilità Ambientale, Università di Parma and INSTM Udr Parma, Parco Area delle Scienze 17/A, 43124 Parma, Italy.

<sup>††</sup> Dipartimento di Ingegneria e Architettura, Università di Parma, Parco Area delle Scienze 181/A, 43124 Parma, Italy.

<sup>‡‡</sup> Corporate R&D, Alfasigma S.p.A., Via Pontina km 30,400, 00071 Pomezia, Italy.

E-mail addresses: [alessia.ciogli@uniroma1.it](mailto:alessia.ciogli@uniroma1.it); [ilaria.dacquarica@uniroma1.it](mailto:ilaria.dacquarica@uniroma1.it)



## ABSTRACT

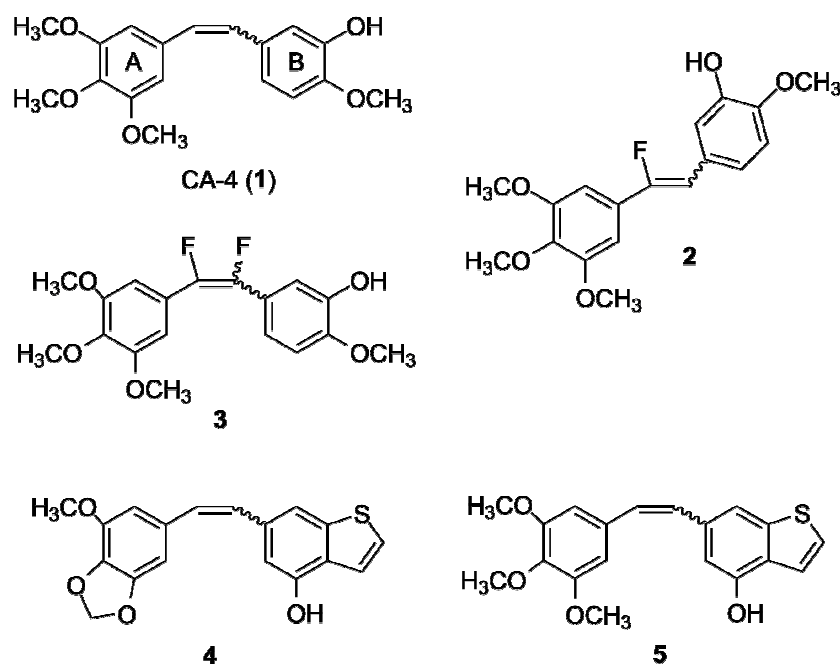
As an extension of our studies on the multifaceted properties of *C*-alkylated resorc[4]arenes, we planned to immobilize on a solid support resorc[4]arenes with C<sub>11</sub>-long side chains in the lower rim. To this purpose, we synthesized two conformationally diverse resorc[4]arenes containing a bromoundecyl moiety in the four axial pendants. The cone stereoisomer **6a** (30% yield) was selected for the reaction with an aminopropylated silica gel (APSG) obtained from spherical Kromasil Si 100, 5 μm particles, to give the corresponding immobilized SP-C<sub>11</sub>-resorc[4]arene system. The resulting polar-embedded stationary phase was fully characterized and investigated in the HPLC discrimination of the *E/Z* stereoisomers of naturally occurring and semi-synthetic combretastatins, a family of (*Z*)-stilbene anticancer drugs. The chair stereoisomer **6b** (20% yield), when submitted to X-ray diffraction analysis, showed a noteworthy self-assembly in the crystal lattice, with intercalated hydrophobic and polar layers as a result of intermolecular Br...O halogen-bond interactions, according to a unique stacking motif.

The potential and versatility of the SP-C<sub>11</sub>-resorc[4]arene stationary phase were shown as well in the separation of highly polar natural products (namely, flavonoids), under reversed-phase (RP) conditions, and of fullerenes C<sub>60</sub> and C<sub>70</sub>, by using apolar solvents as mobile phases.

## INTRODUCTION

One of the most important classes of anticancer drugs is that made by the microtubule-targeting antimitotic agents, which are classified into two main groups: the microtubule-stabilizing (for example, paclitaxel) and the microtubule-destabilizing (e.g., Vinca alkaloids) agents.<sup>1</sup> Combretastatin A4 (CA-4, see Figure 1), which is a naturally occurring (*Z*)-stilbene isolated in 1989 from *Combretum caffrum*,<sup>2</sup> belongs to the second group, and binds to β-tubulin in the so-called colchicine domain, displaying a minor toxicity than the Vinca alkaloids or paclitaxel.<sup>1,3</sup> Despite its potency as anticancer agent, CA-4 did not get approval for therapeutic use because of its low solubility in aqueous media, poor oral bioavailability, short half-life and in vivo double-bond isomerization (from *Z* to *E*); the latter feature, in particular, causes the loss of affinity for β-tubulin, and hence the loss of cytotoxicity.<sup>3</sup> For these reasons, water-soluble derivatives such as combretastatin A-4 phosphate (CA-4P or fosbretabulin)<sup>4</sup> and heterocycle-bridged combretastatin A analogues<sup>5-7</sup> have recently entered clinical trials. More recently, a series of *N*-acylhydrazone derivatives of CA-4 were designed and synthesized

1  
2  
3 on the basis of docking studies,<sup>8</sup> and one of them showed an improved selectivity with respect to the  
4 lead compound, CA-4, toward cancer cells.  
5  
6  
7



32 **Figure 1.** Chemical structures of combretastatin A4 (1) and of some semi-synthetic derivatives (2–5)  
33 analyzed on the SP-C<sub>11</sub>-resorc[4]arene stationary phase.  
34  
35

36  
37 A series of fluorinated analogues of combretastatins have also been synthesized by replacing the  
38 hydroxyl group<sup>9,10</sup> on the B-ring, as well as the methoxy group(s) on the A-ring.<sup>11</sup> The influence of  
39 fluorine substitution on the double bond of combretastatins was also explored by synthesizing *de*  
40 *novo* a small library of derivatives where one (monofluorostilbene) or both (difluorostilbene) of the  
41 double bond hydrogen atoms were replaced by fluorine.<sup>12</sup> More recently, novel fluoro-analogs of  
42 combretastatin CA-4 were synthesized featuring CF<sub>3</sub>-, CF<sub>3</sub>O-, or CF<sub>2</sub>OH-groups instead of the methoxy  
43 group in the B-ring and they have been evaluated for their cytotoxicity against drug-sensitive and  
44 multidrug-resistant cancer cell lines.<sup>13</sup>  
45  
46  
47  
48  
49  
50  
51

52 The stereochemistry of the central double bond in combretastatins is being the subject of some very  
53 recent studies where it has been addressed as a photoactivatable tool that can be switched between  
54 a more potent and a less potent form depending on light, in a fully reversible fashion. It has been  
55  
56  
57  
58  
59  
60

1  
2  
3 definitively predicted, in fact, that the affinity of the *cis*-isomer of CA-4 for tubulin is 10,000-fold larger  
4 than that of *trans*-CA-4, by solving the crystal structure of tubulin in complex with *cis*-CA-4.<sup>14</sup>

5  
6 Furthermore, the renewed interest in combretastatins has been raised by the evidence that they can  
7 inhibit angiogenesis,<sup>4</sup> and are therefore being examined for advanced solid tumors in combination  
8 therapies. As an example, fosbretabulin has just completed Phase 2 clinical trials for the treatment of  
9 neovascular age-related macular degeneration (AMD).<sup>15</sup>

10  
11 We became interested in developing a stationary phase for HPLC capable of discriminating the *E/Z*  
12 stereoisomers of combretastatins, and we planned to combine the entrapping properties of  
13 functionalized resorc[4]arenes with a suitable anchorage to a solid support.<sup>16</sup> Notably, whereas many  
14 calixarene-based stationary phases have been developed for HPLC applications,<sup>17–24</sup> the  
15 resorc[4]arene scaffold was much less investigated as selector for liquid chromatography.<sup>25,26</sup>

16  
17 Enantiomerically pure resorcinarenes have indeed been employed as selectors of chiral stationary  
18 phases (CSPs) for gas chromatography.<sup>27,28</sup>

19  
20 The stationary phase that we obtained (namely, SP-C<sub>11</sub>-resorc[4]arene) was fully characterized and  
21 tested in the stereochemical analysis of a series of semi-synthetic combretastatins, under reversed-  
22 phase (RP) conditions. In fact, it has been shown that the stereochemistry of the stilbene scaffold is  
23 crucial for both tubulin binding and cytotoxicity. Afterwards, the potential and versatility of the  
24 stationary phase were shown as well in the analysis of highly polar compounds, such as flavonoids,  
25 under reversed-phase conditions, and of fullerenes C<sub>60</sub> and C<sub>70</sub>, by using apolar mobile phases.

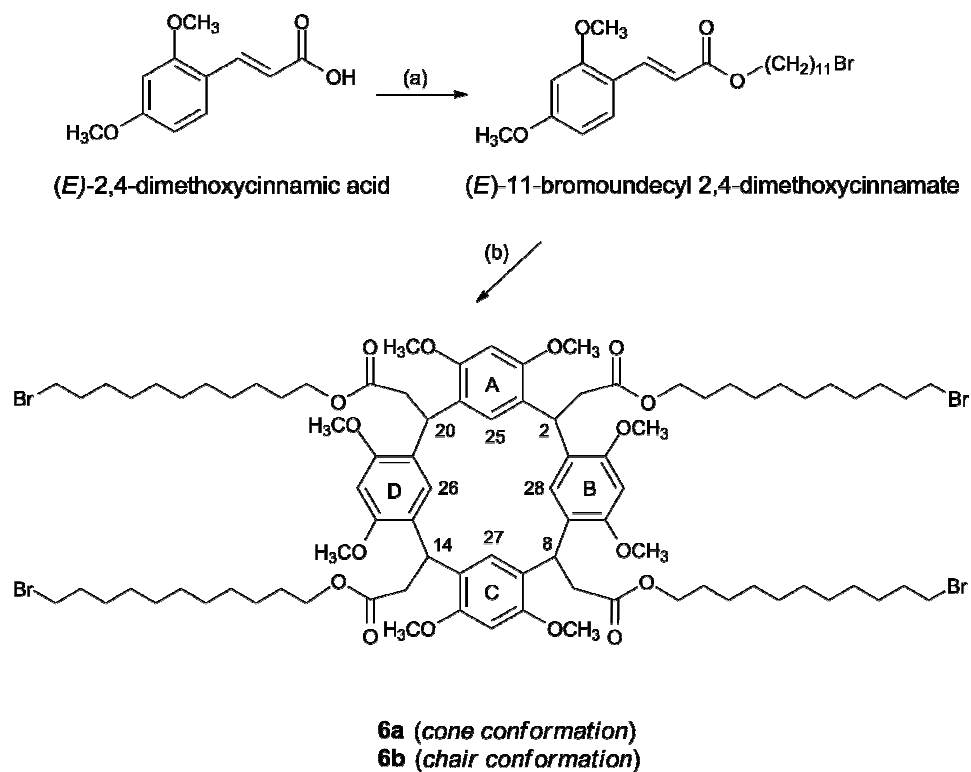
## 26 27 28 29 30 31 32 33 34 35 36 37 38 39 40 **RESULTS AND DISCUSSION**

41  
42 **Synthesis of Bromoundecyl Resorc[4]arenes 6a and 6b.** (*E*)-2,4-Dimethoxycinnamic acid was treated  
43 with 11-bromoundecanol (molar ratio 1:1.2) in dry dichloromethane (DCM), in the presence of 1,3-  
44 dicyclohexylcarbodiimide (DCC) and 4-(dimethylamino)pyridine (DMAP), to give the corresponding  
45 (*E*)-11-bromoundecyl ester as a white solid (74% yield) after purification by silica-gel column  
46 chromatography (Scheme 1). Treatment of (*E*)-11-bromoundecyl 2,4-dimethoxycinnamate with  
47 BF<sub>3</sub>·Et<sub>2</sub>O (molar ratio 1:2) in chloroform under reflux afforded in 50% yield two stereoisomeric  
48 resorc[4]arene bromoundecyl esters, which, after purification by silica-gel column chromatography  
49 and crystallization were shown to be in the cone (**6a**) and chair (**6b**) configurations. The structures of  
50  
51  
52  
53  
54  
55  
56  
57  
58  
59  
60

1  
2  
3 stereoisomers **6a** and **6b** were confirmed by  $^1\text{H}$  and  $^{13}\text{C}$  NMR spectroscopy and by electrospray  
4 ionization high-resolution mass spectrometry (ESI-HRMS).  
5

6  
7 The distribution pattern of the signals (one signal per type of carbon or proton) in the  $^1\text{H}$  and  $^{13}\text{C}$  NMR  
8 spectra of **6a** (30% yield) is typically in agreement with a  $C_{4v}$  symmetry, that is a cone conformation  
9 with all-*cis* pseudo-axial substituents, resulting from an equilibrium between two flattened-cone  
10 forms with  $C_{2v}$  symmetry.<sup>29,30</sup>  
11  
12

13  
14 In the  $^1\text{H}$  and  $^{13}\text{C}$ -NMR spectra of **6b** (20% yield), instead, the distribution pattern includes two signals  
15 for both the aromatic  $\text{CH}_e$  and  $\text{CH}_i$ , and consequently four signals for the other elements of the  
16 aromatic rings, whereas the methine groups give only one signal. Furthermore, the signals for two  
17 protons, namely  $\text{H}_{ih}$  (e.g., H-26 and H-28 in Scheme 1) of two almost coplanar aromatic rings (e.g.,  
18 B/D) are moved highfield under the influence of the two other perpendicular aromatic rings (A/C),  
19 which in turn are on opposite sides with respect to the plane B/D. To assign unequivocally the proper  
20 conformation to resorc[4]arene **6b**, we decided to submit it to X-ray diffraction analysis, which  
21 showed that the macrocycle adopts the chair conformation (see below).  
22  
23  
24  
25  
26  
27  
28  
29  
30  
31  
32  
33  
34  
35  
36  
37  
38  
39  
40  
41  
42  
43  
44  
45  
46  
47  
48  
49  
50  
51  
52  
53  
54  
55  
56  
57  
58  
59  
60



**Scheme 1.** Synthesis of bromoundecyl resorc[4]arenes **6a** and **6b**. Reagents and conditions: (a) 11-bromoundecanol, 1,3-dicyclohexylcarbodiimide chloride (DCC), 4-(dimethylamino)pyridine (DMAP), dry DCM, 0 °C → room temperature, 5 h, 74% yield; (b)  $\text{BF}_3 \cdot \text{Et}_2\text{O}$  (molar ratio 1:2),  $\text{CHCl}_3$ , reflux, 20 min, 50% yield.

**X-Ray Diffraction Analysis of Bromoundecyl Resorc[4]arene 6b.** The molecular structure of resorc[4]arene **6b** is given in Figure 2. By assuming as reference plane R the weighed least squares plane that passes through the four bridged methine atoms of the macrocycle, the calculation of the resulting dihedral angles  $\delta^{31}$  allowed to show that the aromatic rings B and B' are almost coplanar with the R plane, whereas A and A' are almost orthogonal to it, but on opposite sides (see Table 1). Moreover, the conformation of **6b** has been assigned without ambiguity following a procedure already reported,<sup>32,33</sup> based on the use of the conformational parameters  $\varphi$  and  $\chi$  (reported in Table 1). The sequence of signs of the calculated  $\varphi$  and  $\chi$  values (+,-,+,-,+,-) unambiguously indicates that **6b** adopted a chair conformation. Furthermore, being the macrocycle centrosymmetric, the symbolic representation of the molecular conformations becomes  $C_i +-,+,-$ .

1  
2  
3 With such a conformation of the macrocycle, the four ester chains with their terminal bromine atoms  
4 attached to the A and A' rings are extended almost perpendicular to the reference plane R, similarly  
5 to what we found for a C11-long resorc[4]arene ending with a vinylidene group, which we have  
6 recently synthesized as a suitable substrate for olefin metathesis reactions.<sup>34</sup> However, in this case,  
7 the presence of terminal bromine atoms leads to a different self-assembly of resorc[4]arene **6b** in the  
8 crystal lattice, the structure-directing factor for the formation of a "secondary structure" being the  
9 halogen-bond (XB) of the Br...O type, and this is not unexpected. In fact, short halogen-oxygen  
10 interactions have been recently exploited in the design of supramolecular assemblies,<sup>35</sup> and different  
11 architectures based on a resorc[4]arene scaffold have been built by halogen-bond crystal engineering.<sup>36-</sup>  
12  
13  
14  
15  
16  
17  
18  
19  
20

21 As shown in Figure 3, single molecules of resorc[4]arene **6b** proved to be linked by infinite zig-zag  
22 one-dimensional ribbons, in which each molecule can behave as donor and acceptor of Br...O  
23 halogen-bond at the same time. In fact, one ester chain is linked by its terminal bromine atom to the  
24 carbonyl oxygen (O<sub>C=O</sub>) of the resorc[4]arene molecule which is 3.327(8) Å from it and, symmetrically,  
25 the same ester chain is linked via its O<sub>C=O</sub> group to the bromine atom of the adjacent resorc[4]arene,  
26 the R-Br...O angle being equal to 174.0(1)°.  
27  
28  
29  
30  
31  
32  
33  
34  
35  
36  
37  
38  
39  
40  
41  
42  
43  
44  
45  
46  
47  
48  
49  
50  
51  
52  
53  
54  
55  
56  
57  
58  
59  
60

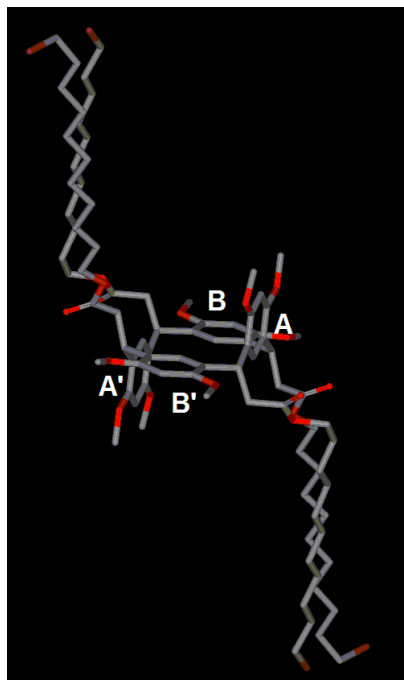


**Figure 2.** Stick view of bromoundecyl resorc[4]arene **6b**. Colors are as follows: C, grey; O, red; Br, light brown. Hydrogen atoms were omitted for clarity.

**Table 1.** Dihedral angles  $\delta$  and conformational parameters  $\varphi$  and  $\chi$  in the molecular structure of bromoundecyl resorc[4]arene **6b**.

Rings	$\delta$ ( $^\circ$ )	Rings	$\varphi$ ( $^\circ$ )	$\chi$ ( $^\circ$ )
R–A' <sup>(a)</sup>	89.92(6)	B–A' <sup>(a)</sup>	155.02(8)	-80.04(7)
R–B' <sup>(a)</sup>	185.46(8)	A'–B'	74.22(8)	-144.76(8)
R–A	270.08(8)	B'–A	-155.02(8)	80.05(7)
R–B	174.54(8)	A–B	-74.22(8)	144.76(8)

(a) Primed aromatic rings are related to unprimed by the center of symmetry. R is the weighed least squares plane that passes through the four bridged methine atoms of the macrocycle. Estimated standard deviations (ESD) are reported in parentheses.

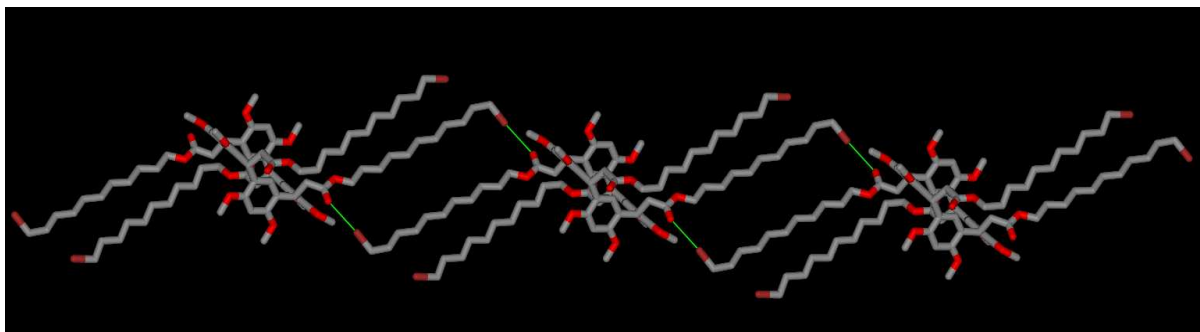


**Figure 3.** Stick view of the self-assembly of bromoundecyl resorc[4]arene **6b** as infinite zig-zag chains in the crystal lattice. Colors are as follows: C, grey; O, red; Br, light brown. Intermolecular Br...O halogen bonds are evidenced by green lines. Hydrogen atoms were omitted for clarity.

Finally, the infinite one-dimensional ribbons are packed in the crystal lattice yielding alternate sequences of polar and apolar layers according to the stacking motif shown in Figure S1 of the Supporting Information. We are currently investigating the potential ability of bromoundecyl resorc[4]arene **6b** to behave as a biomimetic membrane device to be employed in the development of drug delivery systems. Moreover, preliminary studies have shown that bromoundecyl resorc[4]arenes, when added with  $\text{NOBF}_4$  salt, are capable of forming stable 1:1 nitrosonium ( $\text{NO}^+$ ) charge-transfer complexes, and therefore could be used as ( $\text{NO}^+$ ) transfer agents.

**Immobilization of Bromoundecyl Resorc[4]arene 6a on Silica Gel.** We decided to immobilize the cone stereoisomer **6a** on silica gel rather than **6b** because it features the simplest pattern of substituents, i.e., all the four side chains are placed in the same side of the macrocycle (or *rccc*), which forces it to assume a bowl-like shape. In this way, we expected to benefit of a selector which could have shown some recognition behavior at the receptorial level.

We exploited the reactivity of amino-terminated organosilanes with the bromine-ending side chains of the macrocycle. To this purpose, spherical silica-gel microparticles (Kromasil SP-100-5P) were functionalized with (3-aminopropyl)triethoxysilane to give the corresponding 3-aminopropylated silica gel (APSG), which was afterwards submitted to end-capping with 1-(trimethylsilyl)imidazole (TMSI). The surface coverage calculated for the APSG (see Table 2) was  $2.52 \mu\text{mol}/\text{m}^2$  (based on the nitrogen content).

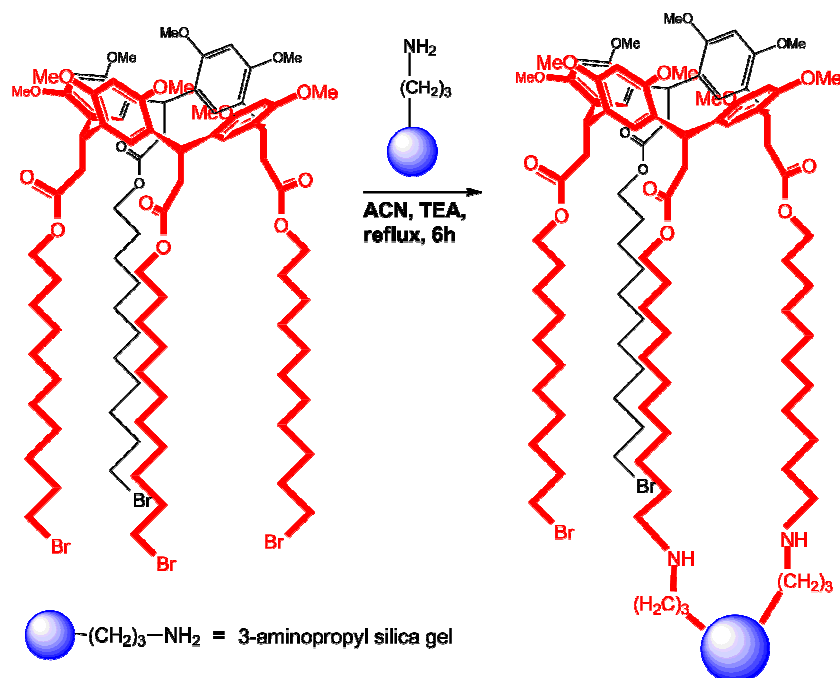
1  
2  
3 Bromoundecyl resorc[4]arene **6a** readily reacted with the above-mentioned APSG, giving the  
4 corresponding SP-C<sub>11</sub>-resorc[4]arene stationary phase (Scheme 2) after refluxing in acetonitrile and  
5 TEA for 6 hours. The grafting reactions, as typically happens in the synthetic protocols for bonded  
6 stationary phases, were monitored by both FT-IR spectroscopy and elemental analysis of the step-by-  
7 step modified silica gels, after appropriate washes. In the last step of the synthetic pathway, the use  
8 of acetonitrile as washing solvent has allowed the removal of the unreacted ligand, whereas intensive  
9 washes with methanol/water assured the disruption of potential physical adsorption phenomena.  
10 Thus, the surface-linking of the resorc[4]arene was first confirmed by the appearance of FT-IR bands  
11 at 1735, 1612, and 1506 cm<sup>-1</sup> (see Figure S2 of the Supporting Information). Afterwards, elemental  
12 analysis of the final SP-C<sub>11</sub>-resorc[4]arene stationary phase (see Table 2) gave a resorc[4]arene loading  
13 equal to 0.28 μmol/m<sup>2</sup> (based on the carbon content), which is comparable with the coverage data  
14 obtained in the literature for the surface linking of calix[*n*]arenes (*n* = 4, 6, 8) and resorcinarenes,  
15 albeit featuring different functionalities.<sup>17–26</sup> Finally, based on the bromine content found on the  
16 phase, we can state that about 2 over 4 arms has statistically been attached to the aminopropylated  
17 silica gel. The SP-C<sub>11</sub>-resorc[4]arene stationary phase obtained was packed into a stainless-steel  
18 column (250 × 4.0 mm I.D.) and characterized as described below.  
19  
20  
21  
22  
23  
24  
25  
26  
27  
28  
29  
30  
31  
32  
33

34 **Table 2.** Surface coverage data for the immobilization of bromoundecyl resorc[4]arene **6a** on Kromasil  
35 Si 100, 5 μm silica particles (specific surface area: 340 m<sup>2</sup>/g).  
36  
37  
38  
39

Material	C (%)	H (%)	N (%)	Br (%)	μmol/g	μmol/m <sup>2</sup>
Kromasil APSG	3.57	1.28	1.08	–	856 <sup>(a)</sup>	2.52 <sup>(a)</sup>
SP-C <sub>11</sub> -resorc[4]arene	11.45	2.03	1.03	1.31	96 <sup>(b)</sup>	0.28 <sup>(b)</sup>

40  
41  
42  
43  
44  
45  
46  
47  
48 (a) Calculation was based on the nitrogen content.

49 (b) Calculation was based on the carbon content.  
50  
51  
52  
53  
54  
55  
56  
57  
58  
59  
60



**Scheme 2.** Immobilization of bromoundecyl resorc[4]arene **6a** (cone conformation) on Kromasil Si 100, 5  $\mu\text{m}$  silica particles. Surface coverage: 0.28  $\mu\text{mol}/\text{m}^2$  (based on carbon). The sketch represents one plausible structure for the 2-armed attachment of the macrocycle on silica gel.

**Characterization of the SP-C<sub>11</sub>-Resorc[4]arene Column.** The hydrophobicity and the chromatographic efficiency of the SP-C<sub>11</sub>-resorc[4]arene column were evaluated by analyzing a mixture of aromatic hydrocarbons (nitrobenzene, toluene, biphenyl, and naphthalene), using water/acetonitrile 50:50 (v/v) as eluent, at a flow-rate of 1.0 mL/min at 25 °C, and UV detection at 214 nm (see Figure S3 of the Supporting Information). For comparative purposes, the same mixture was analyzed on a Phenomenex Luna C18 column and on a lab-packed RP-C8 column featuring the same geometries as the SP-C<sub>11</sub>-resorc[4]arene column. On the basis of the retention behavior shown by the SP-C<sub>11</sub>-resorc[4]arene column, we assume that the column possesses an hydrophobicity more similar to a C8-length column than to a C18-length. In fact, the retention factors ( $k'$  in Table 3) measured on the SP-C<sub>11</sub>-resorc[4]arene column were dramatically smaller than those obtained on the RP-C18 column used for comparison, particularly for biphenyl and naphthalene, where they dropped from 10.08 and 16.78 to 2.79 and 3.62, respectively. The retention factors for nitrobenzene and toluene obtained on the SP-C<sub>11</sub>-resorc[4]arene column were slightly lower than those measured on the RP-C8 one, whereas we

found half values for the two above-mentioned polycyclic aromatic hydrocarbons (i.e., from 4.20 and 6.26 to 2.79 and 3.62, respectively).

With regard to the nitrobenzene/toluene selectivity, only the SP-C<sub>11</sub>-resorc[4]arene column proved capable of separating the two benzene derivatives, which underwent instead peak coalescence on both the conventional reversed-phase columns (see Table 3).

**Table 3.** Retention factors ( $k'$ ) and number of theoretical plates per meter of column (N/m) measured on the SP-C<sub>11</sub>-resorc[4]arene column and comparison with RP-C8 and RP-C18 columns.<sup>(a)</sup>

Column	nitrobenzene		toluene		biphenyl		naphthalene	
	$k'$	N/m	$k'$	N/m	$k'$	N/m	$k'$	N/m
SP-C <sub>11</sub> -resorc[4]arene	1.37	48,400	1.62	52,000	2.79	53,000	3.62	53,200
RP-C8	1.77	58,400	1.77	58,400	4.20	57,400	6.26	56,500
RP-C18	3.02	45,400	3.02	45,400	10.08	47,400	16.78	46,500

(a) Conditions: water/acetonitrile = 50:50 (v/v), flow-rate = 1.0 mL/min, T = 25 °C, UV detection at 214 nm. Columns geometry: 250 × 4.0 mm I.D. (SP-C<sub>11</sub>-resorc[4]arene and lab-packed RP-C8); 250 × 4.6 mm I.D. (Phenomenex Luna C18).

In addition to the hydrophobicity test, the ability of the SP-C<sub>11</sub>-resorc[4]arene phase to discriminate between two molecules differing by a single methylene group was evaluated, according to the methylene selectivity concept.<sup>41</sup> To this purpose, we first analyzed on the SP-C<sub>11</sub>-resorc[4]arene column the homologous series of alkylbenzenes from toluene to pentylbenzene (eluent: water/acetonitrile 50:50, v/v), and then we plotted the logarithm of the retention factors ( $\log k'$ ) obtained versus the number of methylene groups (Figure 4). The slope of the linear regression line yielded the methylene selectivity value for the SP-C<sub>11</sub>-resorc[4]arene phase ( $\alpha_{\text{CH}_2} = 0.10$ ), which proved to be slightly smaller than that obtained for the lab-packed RP-C8 phase used for comparison (i.e., 0.17). These findings are in agreement with the results obtained in the above-discussed retention behavior evaluation of the SP-C<sub>11</sub>-resorc[4]arene phase.

With regard to the chromatographic efficiency of the SP-C<sub>11</sub>-resorc[4]arene column, we have calculated, for the more retained peak (i.e., naphthalene,  $k' = 3.62$ ) a number of theoretical plates per meter of column (N/m) equal to 53,200 (see Table 3).

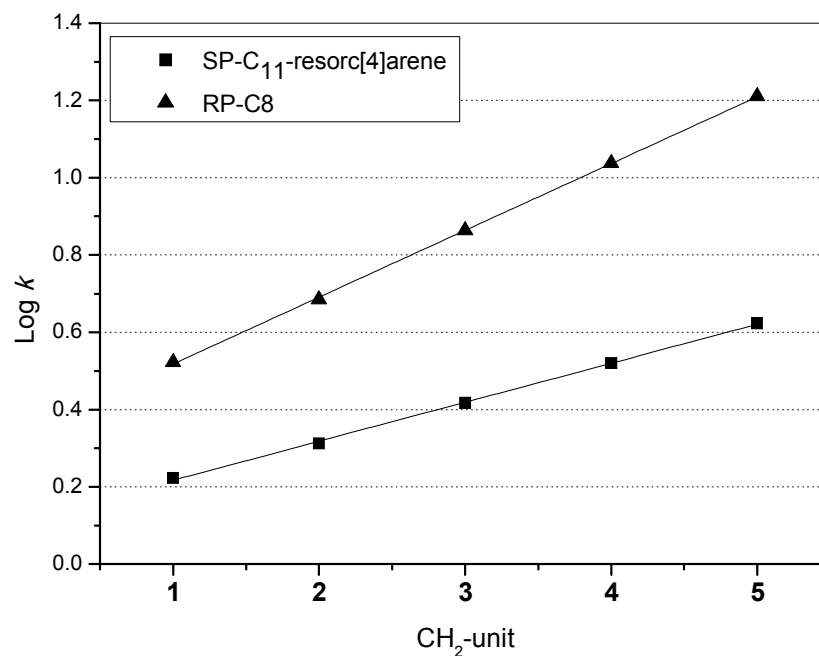


**Figure 4.** Methylene (CH<sub>2</sub> unit) selectivity evaluation for the SP-C<sub>11</sub>-resorc[4]arene (■) column and comparison with the lab-packed RP-C8 (▲) column. Sample mixture: 1 = toluene, 2 = ethylbenzene, 3 = propylbenzene, 4 = butylbenzene, 5 = pentylbenzene. Conditions: water/acetonitrile = 50:50 (v/v), flow-rate = 1.0 mL/min, T = 25 °C, UV detection at 214 nm. Linear regression data:  $y = 0.10x + 0.12$ ,  $r^2 = 0.9996$  (SP-C<sub>11</sub>-resorc[4]arene column);  $y = 0.17x + 0.34$ ,  $r^2 = 0.9999$  (RP-C8 column).

We conclude that the SP-C<sub>11</sub>-resorc[4]arene material can be described as a unique resorc[4]arene-based polar-embedded stationary phase, with an ester functionality bridging between the aromatic cavity and the C<sub>11</sub>-alkyl chain. The phase places itself within conventional C8 and C18 alkyl-bonded phases, with improved selectivity towards substituted aromatics and good peak shapes and efficiencies.

**Applications of the SP-C<sub>11</sub>-Resorc[4]arene Column: Analysis of Combretastatins.** The SP-C<sub>11</sub>-resorc[4]arene column, once characterized as above described, was tested in the separation of the

1  
2  
3 *E/Z* stereoisomers of combretastatin A4 (**1**) and of some semi-synthetic derivatives (**2–5**), whose  
4 chemical structures are reported in Figure 1. Beside the naturally occurring CA-4 (compound **1**), we  
5 included in the investigation two fluorinated analogues, previously prepared by replacement of one  
6 (compound **2**) or both (compound **3**) of the olefinic hydrogen atoms,<sup>12</sup> and two benzothiophen  
7 heterocycles (compounds **4** and **5**), conceived as structural analogues on the A-ring and B-ring.<sup>42,43</sup>

8  
9  
10 Notably, in the benzothiophen analogue **4**, two methoxyl groups on the A-ring are blocked in the  
11 formation of a dioxolane ring (namely, a 3,4-methylenedioxy ring system) which is a common  
12 structural feature with another naturally occurring combretastatin (i.e., combretastatin A-2).<sup>44</sup>

13  
14 To develop a suitable chromatographic method capable of separating the two *E/Z* stereoisomers of  
15 compounds **1–5**, we needed to access to diastereomerically enriched samples, where both the two  
16 stereoisomers could be available. To this purpose, we exploited a photochemical isomerization of  
17 compounds **1–5**, following a previously published three-step protocol<sup>42</sup> and obtained  
18 diastereomerically enriched mixtures which were submitted to chromatography on the SP-C<sub>11</sub>-  
19 resorc[4]arene column (see Figure 5 for typical chromatograms).

20  
21 Retention (*k'*) and diastereoselectivity ( $\alpha$ ) data, collected using water/acetonitrile = 50/50 (v/v) as  
22 mobile phase under isocratic elution, are summarized in Table 4. They showed that the naturally  
23 occurring combretastatin A-4 is the less retained compound on the SP-C<sub>11</sub>-resorc[4]arene column (*k'* =  
24 3.04 for the first eluting diastereoisomer), which yielded as well the minimum  $\alpha$  value (i.e., 1.30)  
25 between the two *E/Z* stereoisomers. According to this way of thinking, the most retained analyte (i.e.,  
26 combretastatin **4**, *k'* = 5.23 for the first eluting diastereoisomer) gave the highest discrimination  
27 between the two *E/Z* diastereoisomers ( $\alpha$  = 1.67), followed by combretastatin **5** ( $\alpha$  = 1.60) which  
28 shares with it the same benzothiophene moiety.

29  
30 The progressive incorporation of the fluorine atoms on the double-bond framework produced an  
31 increase in retention (*k'* of the first eluting diastereoisomer ranging from 3.04 for the native CA-4 to  
32 3.58 for the monofluorinated analogue **2** and 4.81 for the difluoro analogue **3**), which is in agreement  
33 with the increased lipophilicity of the fluorinated molecules. The increase in lipophilicity achieved by  
34 fluoroalkylation of combretastatins has been conceived to increase the drug-target interactions. For  
35 the sake of clarity, it is worth pointing out that the stereochemistry of the fluorinated analogues has  
36 been assigned by <sup>19</sup>F-NMR spectroscopy.<sup>12</sup>

Compound **5** showed a retention behavior ( $k' = 3.69$ ) intermediate between the monofluorinated and difluorinated combretastatins, while the introduction of the dioxolane system on the A-ring (compound **4**) led to a greater affinity for the stationary phase ( $k' = 5.23$ ).

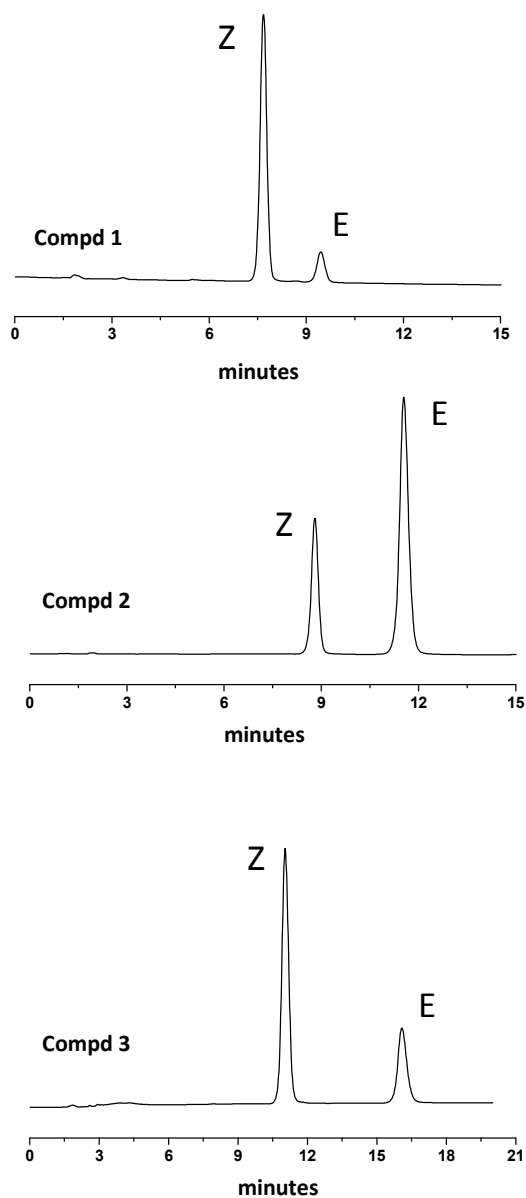


**Figure 5.** Chromatographic separations of the naturally occurring combretastatin A-4 (compound **1**) and of its monofluorinated (compound **2**) and the difluorinated (compound **3**) analogues<sup>12</sup> on the SP-C<sub>11</sub>-resorc[4]arene column (250 × 4.0 mm I.D.). Conditions: water/acetonitrile = 50:50 (v/v), flow-rate = 1.0 mL/min, T = 25 °C, UV detection at 300 nm. For the chemical structures of **1–3**, see Figure 1.

Finally, thanks to the availability of diastereomerically enriched mixtures of combretastatins, we were also able to establish that the (*E*) diastereoisomer is the one preferentially more retained by the immobilized resorc[4]arene (see Table 4). This means that a stronger interaction with the macrocycle likely occurs when the hydrogen or fluorine atoms of the double bond are in a *trans*-arrangement. In fact, it has been demonstrated, for a similar long-chain resorc[4]arene,<sup>34</sup> that such macrocycles behave as good acceptors for CH- $\pi$  interactions, where the reciprocal orientations of the resorc[4]arene core and the olefin counterpart play a pivotal role. Thanks to the occurrence of such interactions, the SP-C<sub>11</sub>-resorc[4]arene column offered better performances in the separation of the *E/Z* stereoisomers of combretastatins when compared to a conventional Inertsil C18, 5  $\mu$ m (250  $\times$  4.6 mm I.D.) column used under the same chromatographic conditions (data not shown). Notably, the order of elution of the *E/Z* stereoisomers on the SP-C<sub>11</sub>-resorc[4]arene, checked on the basis of their absorbance maxima in the UV spectra,<sup>45</sup> proved to be opposite to that already found on a C18 reversed-phase column for combretastatin A-4,<sup>45</sup> using a mixture of water/acetonitrile 60/40 acidified with 0.5% formic acid as the eluent.

**Table 4.** Chromatographic data for the separation of the *E/Z* stereoisomers of combretastatins **1–5** (Figure 1) on the SP-C<sub>11</sub>-resorc[4]arene column.<sup>(a)</sup>

Compd	$k'_1$ <sup>(b)</sup>	$k'_2$ <sup>(c)</sup>	$\alpha$ <sup>(d)</sup>	Config. <sup>(e)</sup>
<b>1</b>	3.04	3.95	1.30	( <i>Z</i> )
<b>2</b>	3.58	5.08	1.42	( <i>Z</i> )
<b>5</b>	3.69	5.90	1.60	( <i>Z</i> )
<b>3</b>	4.81	7.45	1.55	( <i>Z</i> )
<b>4</b>	5.23	8.73	1.67	( <i>Z</i> )

(a) Conditions: water/acetonitrile = 50:50 (v/v), flow-rate = 1.0 mL/min, T = 25 °C, UV detection at 300 nm. (b) Retention factor of the first eluting diastereoisomer. (c) Retention factor of the second eluting diastereoisomer. (d) Diastereoselectivity factor. (e) Absolute configuration of the first eluting diastereoisomer, attributed on the basis of the absorbance maxima in the UV spectra.<sup>45</sup>

1  
2  
3 **Applications of the SP-C<sub>11</sub>-Resorc[4]arene Column: Analysis of Flavonoids and Fullerenes.** With the  
4 aim of broadening the application field of the SP-C<sub>11</sub>-resorc[4]arene stationary phase and further  
5 demonstrating its potential application in the separation of a miscellany of molecules, we investigated  
6 other classes of compounds, such as that of flavonoids, which are highly polar natural products, and  
7 two members of the fullerenes family, i.e., C<sub>60</sub> and C<sub>70</sub>.  
8  
9

10 A standard mixture of four flavonoids from *Passiflora incarnata* L. (i.e., saponarin, vitexin, isovitexin  
11 and apigenin) available from previous studies<sup>46,47</sup> was baseline separated on the SP-C<sub>11</sub>-resorc[4]arene  
12 column using a gradient elution with the following mobile phases: (A) = water/acetonitrile = 75/25  
13 (v/v) + 2% acetic acid and (B) = acetonitrile/2-propanol = 75/25 (v/v) + 2% acetic acid (see Figure 6).  
14 Good peak shapes and efficiencies were achieved for the flavonoid samples, comparable to those  
15 obtained on conventional RP-18 monolith columns,<sup>46</sup> which are known for their high chromatographic  
16 efficiency and low back-pressure.  
17  
18

19 The SP-C<sub>11</sub>-resorc[4]arene column exhibited good performances under normal-phase (NP) conditions  
20 as well, and this is due to the amphiphilic nature of the selector immobilized on silica gel, which  
21 features an ester polar functionality bridging between the aromatic cavity and the C<sub>11</sub>-aliphatic chain.  
22 Beyond a high selectivity shown towards a mixture of aromatic hydrocarbons (see Figure S4 of the  
23 Supporting Information) using a mobile phase consisting of *n*-hexane/dichloromethane 95/5 = (v/v) +  
24 1% methanol, the resorc[4]arene-based column proved capable of separating a mixture of fullerenes  
25 C<sub>60</sub> and C<sub>70</sub>, using *n*-hexane/toluene = 90/10 (v/v) + 1% ethanol as the eluent (Figure 7).  
26  
27  
28  
29  
30  
31  
32  
33  
34  
35  
36  
37  
38  
39  
40  
41  
42  
43  
44  
45  
46  
47  
48  
49  
50  
51  
52  
53  
54  
55  
56  
57  
58  
59  
60

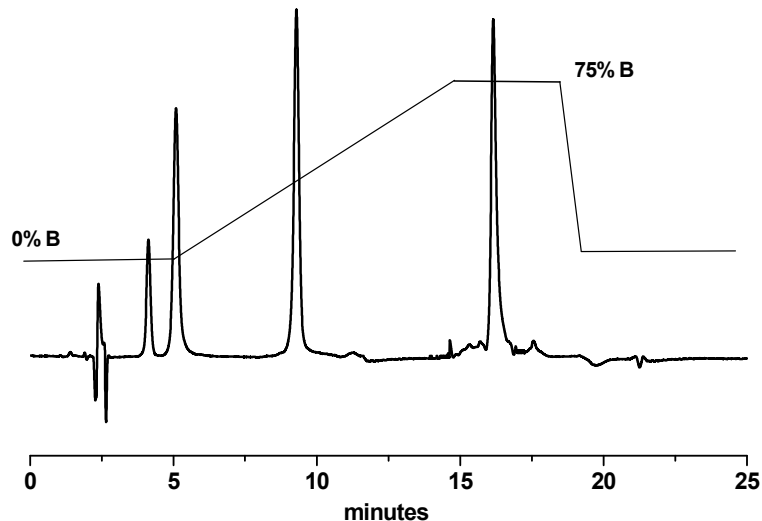


**Figure 6.** Chromatographic separation of flavonoids on the SP-C<sub>11</sub>-resorc[4]arene column (250 × 4.0 mm I.D.). From left to right: saponarin, vitexin, isovitexin and apigenin.

Conditions: water/acetonitrile = 75:25 (v/v) + 2% acetic acid (A), acetonitrile/2-propanol = 75:25 (v/v) + 2% acetic acid (B), flow-rate = 1.0 mL/min, T = 25 °C, UV detection at 254 nm. Gradient elution: from 100% A for 5 min (isocratic), to 75% B in 15 min, at 75% B for 3 min (isocratic), to 100% A over 2 min. The solid line indicates the %B gradient profile.

Since the most suitable stationary phases for the chromatographic separation of fullerene mixtures proved to be those capable of forming  $\pi$ -acid- $\pi$ -basic interactions (e.g., dinitrophenyl-based, dinitroanilinopropyl- or tetraphenylporphyrin-silica), we thought that our SP-C<sub>11</sub>-resorc[4]arene column would have exhibited a good retention and size selectivity towards such close-cage carbon compounds. In fact, the two “buckyballs” accommodated very likely within the hydrophobic cage of the immobilized resorc[4]arene (as we previously observed for a similar hydrophobic macrocycle<sup>48</sup>), and were eluted from the column within ten minutes, with a C<sub>60</sub>/C<sub>70</sub> selectivity factor equal to 1.52. The analytes resulted instead front-eluted when processed on a Hypersil MOS C8 or a bare silica column (data not shown), under the same chromatographic conditions.

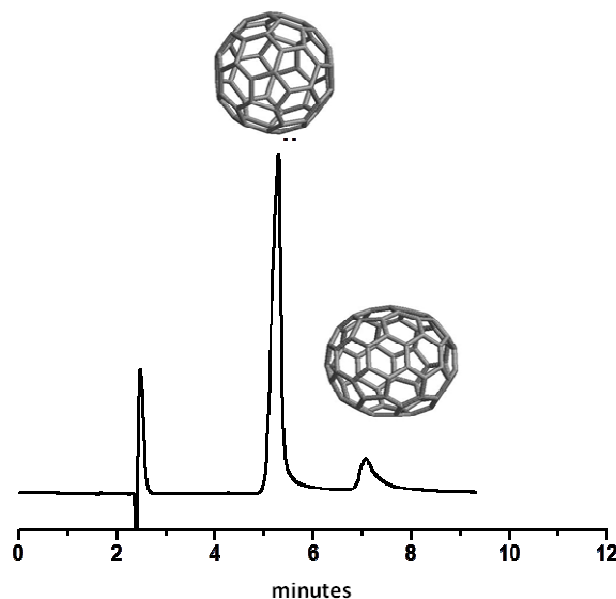


**Figure 7.** Chromatographic separation of a standard mixture (molar ratio 3:1) of fullerenes C60 (first eluting peak) and C70 (second eluting) on the SP-C<sub>11</sub>-resorc[4]arene column (250 × 4.0 mm I.D.). Conditions: *n*-hexane/toluene = 90/10 (v/v) + 1% ethanol, flow-rate = 1.0 mL/min, T = 25 °C, UV detection at 300 nm.

Long-term use of the SP-C<sub>11</sub>-resorc[4]arene stationary phase under both RP and NP conditions yielded relatively high performances after 150 injections in terms of both retention and selectivity factors (see Figure S5 of the Supporting Information). This was taken as a further confirmation of the covalent anchoring of the resorc[4]arene macrocycle to the silica gel, beyond the surface coverage data. The carbon content proved to keep constant as well, by comparing the elemental analysis data checked at the first use of the column with those measured after 150 injections (i.e., it shifted from 11.45% to 10.86%).

## CONCLUSIONS

With the aim of developing a stationary phase for HPLC capable of discriminating the *E/Z* stereoisomers of combretastatins, we synthesized resorc[4]arene stereoisomers **6a** and **6b** containing a bromoundecyl moiety in the four axial pendants by standard tetramerization with BF<sub>3</sub>·Et<sub>2</sub>O as the catalyst. The cone stereoisomer **6a** (30% yield) was selected to be immobilized on silica gel for the all-*cis* configuration of the four side chains which forces the macrocycle to assume a bowl-like shape.

1  
2  
3 As strategy for immobilization, we exploited the reactivity of amino-terminated organosilanes with  
4 the bromine-ending side chains of the macrocycle. The resulting SP-C<sub>11</sub>-resorc[4]arene stationary  
5 phase (with a resorc[4]arene loading equal to 0.28 μmol/m<sup>2</sup>) proved to be a unique resorc[4]arene-  
6 based polar-embedded HPLC stationary phase, with an ester functionality bridging between the  
7 aromatic cavity and the C<sub>11</sub>-alkyl chain. Notably, whereas several functionalized calixarenes have been  
8 employed in the preparation of stationary phases for liquid chromatography as well as capillary  
9 electrophoresis (CE), just a few resorc[4]arene-based HPLC columns have been developed.

10  
11 The SP-C<sub>11</sub>-resorc[4]arene column showed high diastereoselectivity towards the combretastatins  
12 analyzed under reversed-phase conditions, with α values ranging from 1.30 for the naturally occurring  
13 combretastatin A-4 to 1.67 for a benzothiophen analogue. The immobilized resorc[4]arene  
14 established a stronger interaction with the (*E*) diastereoisomer of combretastatins, releasing the  
15 biologically active (*Z*) isomer from the column in a shorter time.

16  
17 Taking into account the renewed interest in combretastatins raised by the evidence that they behave  
18 as a photoactivatable tool (namely, as a photostatin) and inhibit angiogenesis as well, the chance to  
19 check the stereochemistry of the stilbene scaffold seems to be crucial for the design of novel (*Z*-  
20 stilbene-like drug candidates and for the assignment of the stereochemical purity required by the  
21 regulatory authorities.

22  
23 On the other hand, the chair stereoisomer **6b** (20% yield) of bromoundecyl resorc[4]arene, when  
24 submitted to X-ray diffraction analysis, showed a noteworthy self-assembly behavior in the crystal  
25 lattice, with intercalated hydrophobic and polar layers as a result of intermolecular Br...O halogen-  
26 bond interactions. With this dual XB donor/acceptor molecule in hands, we are planning a series of  
27 experiments to evaluate the capability of resorc[4]arene **6b** to mimic biological membranes, where it  
28 may play a role in the entrapment/releasing of gaseous nitrogen oxides (NO<sub>x</sub>).

29  
30 Notably, the SP-C<sub>11</sub>-resorc[4]arene column showed a broad application field, which proved to range  
31 from small molecules with different polarity to close-cage carbon compounds. In the first case, the  
32 resorc[4]arene scaffold behaved as a brush-type selector capable of working under mixed-mode  
33 conditions, by establishing, among others, CH-π interactions with the analytes. In the second case, the  
34 macrocycle proved to be able to accommodate within its hydrophobic cage the fullerenes C<sub>60</sub> and  
35 C<sub>70</sub>, at a receptorial level. This feature would benefit of a deeper and dedicated investigation, which  
36 could be the topic of another article.

## EXPERIMENTAL SECTION

**General Information.** All the reagents were commercial and were used without further purification. Chromatography was carried out on silica gel (230–400 mesh). All the reactions were monitored by thin-layer chromatography (TLC), and silica gel plates with fluorescence F254 were used.  $^1\text{H}$  and  $^{13}\text{C}$  NMR spectra were recorded on a 400 MHz spectrometer. Data for  $^1\text{H}$  NMR are reported as a chemical shift ( $\delta$ , ppm), multiplicity (s = singlet, d = doublet, t = triplet, q = quartet, quint = quintuplet, m = multiplet), coupling constant  $J$  (Hz), integration, and assignment. Data for  $^{13}\text{C}$  are reported as a chemical shift.  $^1\text{H}$  and  $^{13}\text{C}$  NMR spectra were always referenced to a residual  $\text{CHCl}_3$  signal ( $^1\text{H}$ ,  $\delta = 7.26$  ppm;  $^{13}\text{C}$ ,  $\delta = 77.20$  ppm). Melting points were measured in open capillaries on a Büchi Melting Point B-545 apparatus. High-resolution (HR) mass spectra were obtained using an Orbitrap mass spectrometer equipped with an electrospray ionization (ESI) source; capillary temperature 275 °C, spray voltage 3.5 kV; sheath gas (nitrogen) 10 arbitrary units, capillary voltage 65 V, tube lens 125 V.

**Chemicals and Reagents.** Kromasil SP-100-5P silica gel (specific surface area 340  $\text{m}^2/\text{g}$ ) was from Sigma-Aldrich (St. Louis, MO, USA). HPLC grade solvents were 0.45  $\mu\text{m}$  filtered before using. Stainless-steel columns (250  $\times$  4.0 mm I.D.) were supplied by Alltech (IL, USA). A Phenomenex Luna C18, 5  $\mu\text{m}$  (250  $\times$  4.6 mm I.D.) and a lab-packed RP-C8 (250  $\times$  4.0 mm I.D.) columns were employed for comparison.

**Synthesis of (*E*)-11-Bromoundecyl 2,4-Dimethoxycinnamate.** A solution of (*E*)-2,4-dimethoxycinnamic acid (8.0 g, 38.4 mmol) in dry DCM (80 mL) cooled to 0 °C was treated with 11-bromoundecanol (11.6 g, 46.2 mmol), 1,3-dicyclohexylcarbodiimide (9.5 g, 46.0 mmol) and 4-(dimethylamino)pyridine (2.35 g, 19.2 mmol). The resulting reaction mixture was kept stirred for 5h at room temperature. Purification of the crude residue by silica gel column chromatography with chloroform as eluent afforded the title compound (12.5 g, 28.3 mmol, 74%) as a white solid. Mp: 64–66 °C.  $^1\text{H}$  NMR ( $\text{CDCl}_3$ , 400 MHz, 300 K):  $\delta$  (ppm) 7.89 (d,  $J = 16.1$  Hz, 1H, H- $\beta$ ), 7.43 (d,  $J = 8.6$  Hz, 1H, H-6), 6.48 (dd,  $J = 8.5$ , 2.3 Hz, 1H, H-5), 6.44–6.40 (m, 2H, H-3, H- $\alpha$ ), 4.17 (t,  $J = 6.8$  Hz, 2H,  $\text{OCH}_2$ ), 3.86 (s, 3H,  $\text{OCH}_3$ ), 3.83 (s, 3H,  $\text{OCH}_3$ ), 3.39 (t,  $J = 6.9$  Hz, 2H,  $\text{CH}_2\text{Br}$ ), 1.84 (quint,  $J = 6.8$  Hz, 2H,  $\text{CH}_2\text{CH}_2\text{Br}$ ), 1.68 (quint,  $J = 6.8$  Hz, 2H,  $\text{OCH}_2\text{CH}_2$ ), 1.41 (br m, 4H, 2  $\times$   $\text{CH}_2$ ), 1.28 (br m, 10H, 5  $\times$   $\text{CH}_2$ ).  $^{13}\text{C}$  NMR ( $\text{CDCl}_3$ , 100 MHz, 300 K):  $\delta$

(ppm) 168.17, 162.81, 159.98, 140.08, 130.56, 116.81, 116.32, 105.36, 98.57, 64.53, 55.91, 55.62, 55.61, 35.08, 34.19, 33.00, 29.62, 29.59, 29.56, 29.42, 28.95, 28.91, 28.33, 26.13, 25.62, 24.85. HRMS (ESI/Orbitrap)  $m/z$ :  $[M + H]^+$  Calcd for  $C_{22}H_{33}BrO_4H$  441.1635 (monoisotopic mass); Found: 441.1634.

**Synthesis of Bromoundecyl Resorc[4]arenes 6a and 6b.** An aliquot of  $BF_3 \cdot Et_2O$  (7.0 mL, 56.7 mmol) was added to a solution of (*E*)-11-bromoundecyl 2,4-dimethoxycinnamate (12.5 g, 28.3 mmol) in  $CHCl_3$  (140 mL) under stirring and the reaction mixture was held under reflux for 20 min. After the addition of ice-water, the stirring was continued overnight. The chloroform layer was dried over  $Na_2SO_4$  and the solvent was removed under vacuum. The residue was purified by silica gel column chromatography (DCM/*n*-hexane/ethyl acetate, 70:25:5) to yield bromoundecyl resorc[4]arenes **6a** (3.7 g, 2.1 mmol, 30%) and **6b** (2.5 g, 1.4 mmol, 20%) as white solids.

**Bromoundecyl Resorc[4]arene 6a (Cone Stereoisomer).** White solid, 30% yield. Mp: 91–93 °C.  $^1H$  NMR ( $CDCl_3$ , 400 MHz, 300 K):  $\delta$  (ppm) 6.48 (s br, 4H,  $ArCH_i$ ), 6.28 (s, 4H,  $ArCH_e$ ), 4.94 (t,  $J = 7.6$  Hz, 4H, 4  $\times$  CH), 3.93 (t,  $J = 6.6$  Hz, 8H, 4  $\times$   $OCH_2$ ), 3.61 (s, 24H, 8  $\times$   $OCH_3$ ), 3.38 (t,  $J = 6.8$  Hz, 8H, 4  $\times$   $CH_2Br$ ), 2.80 (d,  $J = 7.5$  Hz, 8H, 4  $\times$   $CH_2CO$ ), 1.83 (quint,  $J = 7.3$  Hz, 8H, 4  $\times$   $CH_2CH_2Br$ ), 1.47 (m br, 8H, 4  $\times$   $CH_2$ ), 1.40 (m, 8H, 4  $\times$   $CH_2$ ), 1.25–1.20 (m, 48H, 24  $\times$   $CH_2$ ).  $^{13}C$  NMR ( $CDCl_3$ , 100 MHz, 300 K):  $\delta$  (ppm) 172.60, 156.18, 125.96, 124.31, 96.50, 64.44, 56.08, 39.22, 34.22, 33.19, 33.01, 29.67, 29.61, 29.48, 28.94, 28.74, 28.35, 26.03. HRMS (ESI/Orbitrap)  $m/z$ :  $[M + Na]^+$  Calcd for  $C_{88}H_{132}Br_4O_{16}Na$  1787.6128; Found: 1787.6169.

**Bromoundecyl Resorc[4]arene 6b (Chair Stereoisomer).** White solid, 20% yield. Mp: 129–131 °C.  $^1H$  NMR ( $CDCl_3$ , 400 MHz, 300 K):  $\delta$  (ppm) 6.79 (s, 2H,  $ArCH_i$ ), 6.45 (s, 2H,  $ArCH_e$ ), 6.38 (s, 2H,  $ArCH_e$ ), 6.17 (s, 2H,  $ArCH_i$ ), 5.02 (dd,  $J = 9.2, 6.5$  Hz, 4H, 4  $\times$  CH), 3.94 (m, 4H, 4  $\times$   $OCH_AH_B$ ), 3.87 (s, 12H, 4  $\times$   $OCH_3$ ), 3.83 (m, 4H, 4  $\times$   $OCH_AH_B$ ), 3.63 (s, 12H, 4  $\times$   $OCH_3$ ), 3.40 (t,  $J = 6.8$  Hz, 8H, 4  $\times$   $CH_2Br$ ), 2.69 (m, 4H, 2  $\times$   $CH_AH_BCO$ ), 2.64 (m, 4H, 2  $\times$   $CH_AH_BCO$ ), 1.84 (quint,  $J = 6.8$  Hz, 8H, 4  $\times$   $CH_2CH_2Br$ ), 1.42 (br m, 16H, 8  $\times$   $CH_2$ ), 1.28–1.21 (m br, 48H, 24  $\times$   $CH_2$ ).  $^{13}C$  NMR ( $CDCl_3$ , 100 MHz, 300 K):  $\delta$  (ppm) 172.61, 156.63, 155.82, 126.67, 125.77, 125.33, 122.75, 97.29, 95.63, 64.38, 56.20, 56.08, 39.68, 34.22, 33.01, 32.97, 29.68, 29.61, 29.49, 28.95, 28.73, 28.35, 26.00. HRMS (ESI/Orbitrap)  $m/z$ :  $[M + Na]^+$  Calcd for  $C_{88}H_{132}Br_4O_{16}Na$  1787.6128; Found: 1787.6169.

1  
2  
3  
4  
5 **Crystallographic Data for Bromoundecyl Resorc[4]arene 6b.** C<sub>88</sub>H<sub>132</sub>Br<sub>4</sub>O<sub>16</sub>, M = 1765.57, crystal  
6 system: monoclinic, space group: *P*-1, a = 12.197(3) Å, b = 18.407(5) Å, c = 10.556(3) Å, α = 99.057(6)°,  
7 β = 99.848(6)°, γ = 98.921(6)°, V = 2265.2(11) Å<sup>3</sup>, Z = 1, ρ<sub>calcd</sub> = 1.294 g/cm<sup>3</sup>, μ = 1.837 mm<sup>-1</sup>. 21834  
8 Reflections collected, 8001 independent reflections (R<sub>int</sub> = 0.0947). Additional crystallographic data,  
9 experimental and refinement parameters are given in the Supporting Information.  
10  
11  
12  
13  
14  
15

16 **Synthesis of the SP-C<sub>11</sub>-Resorc[4]arene Stationary Phase.** A slurry of vacuum-dried (0.1 mbar, 1h, at  
17 150 °C) Kromasil Si 100, 5 μm silica gel (5.0 g) in toluene (120 mL) was heated to reflux, and the  
18 residual water was azeotropically removed. After cooling to room temperature, (3-  
19 aminopropyl)triethoxysilane was added (2.5 mL, 11 mmol) and the mixture was heated to reflux for  
20 4h. After cooling to room temperature, the modified aminopropylated silica gel (APSG) was isolated  
21 by filtration, washed with 50 mL portions of toluene, methanol and dichloromethane and dried at  
22 reduced pressure (90 °C, 0.1 mbar, 1h). Anal. found: C, 3.57; H, 1.28; N, 1.08, corresponding to 856  
23 μmol of aminopropyl groups per gram of unmodified silica-gel (alternatively 2.52 μmol/m<sup>2</sup>), based on  
24 nitrogen.  
25  
26  
27  
28  
29  
30  
31

32 A slurry of 3-aminopropyl silica gel (3.0 g) in toluene (30 mL) containing 1-(trimethylsilyl)imidazole  
33 (TMSI, 1.8 mL) was refluxed and stirred for 4h, under dry atmosphere. The obtained end-capped silica  
34 gel was isolated by filtration and was washed with toluene, methanol, methanol with TEA (1%),  
35 methanol, dichloromethane, and dried under vacuum at 60 °C. Anal. found: C, 3.72; H, 1.44; N, 0.89.  
36  
37 A solution of bromoundecyl resorc[4]arene **6a** (0.71 g, 0.40 mmol), obtained as previously described,  
38 in dry acetonitrile containing 4% of triethylamine (TEA, 50 mL) was added to the end-capped 3-  
39 aminopropyl silica gel (2.5 g), and the mixture was refluxed for 6h, with continuous stirring. The  
40 progress of the reaction was monitored by FT-IR spectroscopy (see below). After cooling to room  
41 temperature, the SP-C<sub>11</sub>-resorc[4]arene phase was isolated by filtration, washed with 20 mL portions  
42 of acetonitrile, methanol, water, methanol and dichloromethane, and dried under reduced pressure  
43 (50 °C, 0.1 mbar, 2h). Anal. found: C, 11.45; H, 2.03; N, 1.03; Br, 1.31 corresponding to 96 μmol of  
44 resorc[4]arene per gram of unmodified silica (alternatively 0.28 μmol/m<sup>2</sup>), based on carbon. FT-IR  
45 (KBr): ν 1735; 1612; 1506; 1465 cm<sup>-1</sup>.  
46  
47  
48  
49  
50  
51  
52  
53  
54  
55  
56  
57  
58  
59  
60

1  
2  
3 **Column Packing and Efficiency Tests.** The SP-C<sub>11</sub>-resorc[4]arene stationary phase was packed into a  
4 stainless-steel column (250 × 4.0 mm I.D.) using a slurry packing procedure already described.<sup>49–51</sup>  
5

6 The hydrophobicity and the chromatographic efficiency of the SP-C<sub>11</sub>-resorc[4]arene column were  
7 evaluated by injecting a mixture of nitrobenzene, toluene, biphenyl, and naphthalene, using  
8 water/acetonitrile 50:50 (v/v) as eluent, at a flow-rate of 1.0 mL/min at 25 °C, and UV detection at  
9 214 nm. The column hold-up time ( $t_0 = 1.9$  min) was determined by the elution time of an unretained  
10 marker (acetone) using acetonitrile as eluent, at a flow-rate of 1.0 mL/min at 25 °C, and UV detection  
11 at 254 nm.  
12  
13  
14  
15  
16  
17  
18

19 **Chromatographic Conditions.** Flow-rate and column temperature were set to 1.0 mL/min and 25 °C,  
20 respectively, in all runs. Reversed-phase (RP) separations of combretastatins **1–5** were carried out by  
21 using a mixture consisting of water/acetonitrile = 50/50 (v/v) as mobile phase under isocratic elution  
22 (pH<sub>app.</sub> = 7.2), whereas for the separation of flavonoids a gradient elution was adopted with the  
23 following mobile phases: (A) = water/acetonitrile = 75/25 (v/v) + 2% acetic acid; (B) = acetonitrile/2-  
24 propanol = 75/25 (v/v) + 2% acetic acid. Gradient profile: start 100% A, 5 min 100% A, 15 min A/B  
25 25/75, 18 min A/B 25/75, 19 min 100% A (end). PDA detection was in the 210–400 nm range. Samples  
26 were dissolved in mobile phase (0.5 mg/mL) or, whether poorly soluble, in methanol.  
27  
28

29 Normal-phase (NP) separation of aromatic hydrocarbons (i.e., benzene, nitrobenzene, methyl  
30 benzoate, acetophenone and 1,3-dinitrobenzene) was carried out by using a mixture consisting of *n*-  
31 hexane/dichloromethane 95/5 = (v/v) + 1% methanol and UV detection at 254 nm.  
32  
33

34 The C<sub>60</sub>/C<sub>70</sub> fullerene mixture was resolved by using *n*-hexane/toluene = 90/10 (v/v) + 1% ethanol as  
35 mobile phase and UV detection at 300 nm.  
36  
37  
38  
39

#### 40 41 42 43 44 45 **ASSOCIATED CONTENT**

46 CCDC 1820772 contains the supplementary crystallographic data for the structure reported (excluding  
47 structure factors) and can be obtained free of charge from The Cambridge Crystallographic  
48 Data Centre via <http://www.ccdc.cam.ac.uk>.  
49

50 The Supporting Information related to this article includes the following: crystal data and structure  
51 refinement for bromoundecyl resorc[4]arene **6b**, copies of NMR and HRMS spectra for (*E*)-11-  
52 bromoundecyl 2,4-dimethoxycinnamate, compounds **6a** and **6b**, FT-IR spectra of the SP-C<sub>11</sub>-  
53  
54  
55  
56  
57  
58  
59  
60

1  
2  
3 resorc[4]arene stationary phase, HPLC efficiency (both under normal-phase and reversed-phase  
4 conditions) and stability tests for the SP-C<sub>11</sub>-resorc[4]arene column.  
5  
6  
7

### 8 **Acknowledgements** 9

10 We thank the financial support from Sapienza Università di Roma, Italy (Funds for Selected Research  
11 Topics 2016 and 2017 and FFABR) and Bilateral Project 2016 between Sapienza Università di Roma  
12 (Italy) and the Universidade Federal de Santa Catarina (Florianopolis, Brazil).  
13  
14

15 Elemental analysis of the stationary phase was performed at the Mikroanalytisches Laboratorium of  
16 the Vienna University, Wien, Austria (analysis report 0418/0473).  
17  
18

19 We gratefully acknowledge Prof. Bruno Botta (Sapienza Università di Roma, Italy) for helpful  
20 discussion of the paper, and Prof. Francesco Gasparrini (Emeritus Professor at Sapienza Università di  
21 Roma, Italy) for his precious support with the development of the resorc[4]arene-based stationary  
22 phase.  
23  
24  
25  
26  
27  
28  
29  
30  
31  
32  
33  
34  
35  
36  
37  
38  
39  
40  
41  
42  
43  
44  
45  
46  
47  
48  
49  
50  
51  
52  
53  
54  
55  
56  
57  
58  
59  
60

## References

- [1] Stanton, R. A.; Gernert, K. M.; Nettles, J. H.; Aneja, R. Drugs that target dynamic microtubules: a new molecular perspective, *Med. Res. Rev.* **2011**, 31, 443–481.
- [2] Pettit, G. R.; Singh, S. B.; Hamel, E.; Lin, C. M.; Alberts, D. S.; Garcia-Kendall, D. Isolation and structure of the strong cell growth and tubulin inhibitor combretastatin A-4, *Experientia* **1989**, 45, 209–211.
- [3] (a) Tron, G. C.; Pirali, T.; Sorba, G.; Pagliai, F.; Busacca, S.; Genazzani, A. A. Medicinal chemistry of combretastatin A-4: Present and future directions, *J. Med. Chem.* **2006**, 49, 3033–3044. (b) Bukhari, S. N. A.; Kumar, G. B.; Revankar, H. M.; Qin, H. -L. Development of combretastatins as potent tubulin polymerization inhibitors, *Bioorg. Chem.* **2017**, 72, 130–147.
- [4] (a) Chaplin, D. J.; Pettit, G. R.; Hill, S. A. Anti-vascular approaches to solid tumour therapy: evaluation of combretastatin A4 phosphate, *Anticancer Res.* **1999**, 19, 189–196. (b) Chaplin, D. J.; Hill, S. A. The development of combretastatin A4 phosphate as a vascular targeting agent, *Int. J. Radiat. Oncol. Biol. Phys.* **2002**, 54, 491–1496. (c) Prisen, V. E.; Honess, D. J.; Stratford, M. R.; Wilson, J.; Tozer, G. M. The vascular response of tumor and normal tissues in the rat to the vascular targeting agent, combretastatin A-4 phosphate, at clinically relevant dose, *Int. J. Oncol.* **2002**, 21, 717–726. (d) West, C. M.; Price, P. Combretastatin A4 phosphate, *Anticancer Drugs* **2004**, 15, 179–187. (e) Ibrahim, M. A.; Do, D. V.; Sepah, Y. J.; Shah, S. M.; Van Anden, E. et al. Vascular disrupting agent for neovascular age related macular degeneration: a pilot study of the safety and efficacy of intravenous combretastatin A-4 phosphate, *BMC Pharmacol. Toxicol.* **2013**, 14, 7–16.
- [5] Wang, L.; Woods, K. W.; Li, Q.; Barr, K. J.; McCroskey, R. W. et al. Potent, orally active heterocycle-based combretastatin A-4 analogues: synthesis, structure-activity relationship, pharmacokinetics, and in vivo antitumor activity evaluation, *J. Med. Chem.* **2002**, 45, 1697–1711.
- [6] Biersack, B.; Effenberger, K.; Schobert, R.; Ocker, M. Oxazole-bridged combretastatin A analogues with improved anticancer properties, *ChemMedChem* **2010**, 5, 420–427.
- [7] Pati, H. N.; Wicks, M.; Holt Jr, H. L.; LeBlanc, R.; Weisbruch, P. et al. Synthesis and biological evaluation of cis-combretastatin analogs and their novel 1,2,3-triazole derivatives, *Heterocycl. Commun.* **2005**, 11, 117–120.

- [8] do Amaral, D. N.; Cavalcanti, B. C.; Bezerra, D. P.; Ferreira, P. M. P.; Castro, R. de P. et al. Docking, synthesis and antiproliferative activity of N-acylhydrazone derivatives designed as combretastatin A4 analogues, *PLoS ONE* **2014**, 9, e85380.
- [9] Lawrence, N. J.; Hepworth, L. A.; Rennison, D.; McGown, A. T.; Hadfield, J. A. Synthesis and anticancer activity of fluorinated analogues of combretastatin A-4, *J. Fluor. Chem.* **2003**, 123, 101–108.
- [10] Gaukroger, K.; Hadfield, J. A.; Lawrence, N. J.; Nolan, S.; McGown, A. T. Structural requirements for the interaction of combretastatins with tubulin: how important is the trimethoxy unit, *Org. Biomol. Chem.* **2003**, 1, 3033–3037.
- [11] Ducki, S.; Mackenzie, G.; Lawrence, N. J.; Snyder, J. P. Quantitative structure-activity relationship (5D-QSAR) study of combretastatin-like analogues as inhibitors of tubulin assembly, *J. Med. Chem.* **2005**, 48, 457–465.
- [12] (a) Giannini, G.; Marzi, M.; Alloatti, D.; Tinti, M. O.; Riccioni, T. et al. Fluorocombretastatin and derivatives thereof. PCT Int. Appl. WO05007603, **2005**. (b) Alloatti, D.; Giannini, G.; Cabri, W.; Lustrati, I.; Marzi, M. et al. Synthesis and biological activity of fluorinated combretastatin analogues, *J. Med. Chem.* **2008**, 51, 2708–2721.
- [13] Zong, Y.; Shea, C.; Maffucci, K.; Ojima, I. Computational design and synthesis of novel fluoro-analogs of combretastatins A-4 and A-1, *J. Fluor. Chem.* **2017**, 203, 193–199.
- [14] Gaspari, R.; Prota, A. E.; Bargsten, K.; Cavalli, A.; Steinmetz, M. O. Structural basis of *cis*- and *trans*-combretastatin binding to tubulin, *Chem* **2017**, 2, 102–113.
- [15] (a) Al-Abd, A. M.; Alamoudi, A. J.; Abdel-Naim, A. B.; Neamatallah, T. A.; Ashour, O. M. Anti-angiogenic agents for the treatment of solid tumors: potential pathways; therapy and current strategies – A review, *J. Adv. Res.* **2017**, 8, 591–605. (b) <https://www.clinicaltrials.gov>.
- [16] (a) Nunziata, A.; Lionetti, G.; Pierri, E.; Botta, B.; Cancelliere, G.; D'Acquarica, I. et al. Synthesis of resorcin[4]arenes and their use to adsorb nitrogen oxides from tobacco smoke. PCT Int. Appl. 2006; 51 pp., WO2006136950, Deposit 28.12.2006. (b) Nunziata, A.; Lionetti, G.; Pierri, E.; Botta, B.; Cancelliere, G.; D'Acquarica, I. et al. Method of reducing the level of nitrogen oxides in a medium by absorption with resorcin[4]arenes. PCT Int. Appl. EP 1738821, Deposit 03.01.2007.
- [17] (a) Friebe, S.; Gebauer, S.; Krauss, G. -J.; Goermar, G.; Krueger, J. HPLC on calixarene bonded silica gels. I. Characterization and applications of the *p*-*tert*-butyl-calix[4]arene bonded material, *J.*

- 1  
2  
3 *Chromatogr. Sci.* **1995**, 33, 281–284. (b) Gebauer, S.; Friebe, S.; Gübitz, G.; Krauss, G.-J. High  
4 performance liquid chromatography on calixarene-bonded silica gels. II. Separations of regio- and  
5 stereoisomers on *p*-tert-butylcalix[n]arene phases, *J. Chromatogr. Sci.* **1998**, 36, 383–387. (c) Gebauer,  
6 S.; Friebe, S.; Scherer, G.; Gübitz, G.; Krauss, G.-J. High performance liquid chromatography on  
7 calixarene-bonded silica gels. III. Separations of *cis/trans* isomers of proline-containing peptides, *J.*  
8 *Chromatogr. Sci.* **1998**, 36, 388–394.  
9  
10 [18] Sokoließ, T.; Menyés, U.; Roth, U.; Jira, T. New calixarene-bonded stationary phases in high-  
11 performance liquid chromatography: comparative studies on the retention behavior and on  
12 influences of the eluent, *J. Chromatogr. A* **2000**, 898, 35–52.  
13  
14 [19] Śliwka-Kaszyńska, M.; Jaszczolt, K.; Witt, D.; Rachoń, J. High-performance liquid chromatography  
15 of di- and trisubstituted aromatic positional isomers on 1,3-alternate 25,27-dipropoxy-26,28-bis-[3-  
16 propyloxy]-calix[4]arene-bonded silica gel stationary phase, *J. Chromatogr. A* **2004**, 1055, 21–28.  
17  
18 [20] Huai, Q. Y.; Zhao, B.; Zuo, Y. M. Preparation and evaluation of an end-capped *p*-tert-butyl-  
19 calix[4]arene-bonded-silica stationary phase for reversed-phase high-performance liquid  
20 chromatography, *Chromatographia* **2004**, 59, 637–645.  
21  
22 [21] Alahmadi, S. M.; Mohamad, S.; Maah, M. J. Synthesis and characterization of mesoporous silica  
23 functionalized with calix[4]arene derivatives, *Int. J. Mol. Sci.* **2012**, 13, 13726–13736.  
24  
25 [22] Chamseddin, C.; Jira, T. Evaluation of the chromatographic performance of conventional; polar-  
26 endcapped and calixarene-bonded stationary phases for the separation of water-soluble vitamins,  
27 *Chromatographia* **2013**, 76, 449–457.  
28  
29 [23] Zadmard, R.; Heydar, K. T.; Imani, M. Separation of amino acids by high performance liquid  
30 chromatography based on calixarene-bonded stationary phases, *J. Chromatogr. Sci.* **2015**, 53, 702–  
31 707.  
32  
33 [24] Narkhede, N.; Uttam, B.; Kandi, R.; Rao, C. P. Silica–calix hybrid composite of allyl calix[4]arene  
34 covalently linked to MCM-41 nanoparticles for sustained release of doxorubicin into cancer cells, *ACS*  
35 *Omega* **2018**, 3, 229–239.  
36  
37 [25] Sokoließ, T.; Menyés, U.; Roth, U.; Jira, T. Separation of *cis*- and *trans*-isomers of thioxanthene  
38 and dibenz[*b*;e]oxepin derivatives on calixarene- and resorcinarene-bonded high-performance liquid  
39 chromatography stationary phases, *J. Chromatogr. A* **2002**, 948, 309–319.  
40  
41  
42  
43  
44  
45  
46  
47  
48  
49  
50  
51  
52  
53  
54  
55  
56  
57  
58  
59  
60

- [26] Ruderisch, A.; Iwanek, W.; Pfeiffer, J.; Fischer, G.; Albert, K.; Schurig, V. Synthesis and characterization of a novel resorcinarene-based stationary phase bearing polar headgroups for use in reversed-phase high-performance liquid chromatography, *J. Chromatogr. A* **2005**, 1095, 40–49.
- [27] Pfeiffer, J.; Schurig, V. Enantiomer separation of amino acid derivatives on a new polymeric chiral resorc[4]arene stationary phase by capillary gas chromatography, *J. Chromatogr. A* **1999**, 840, 145–150.
- [28] Ruderisch, A.; Pfeiffer, J.; Schurig, V. Synthesis of an enantiomerically pure resorcinarene with pendant L-valine residues and its attachment to a polysiloxane (Chirasil-Calix), *Tetrahedron: Asymm.* **2001**, 12, 2025–2030.
- [29] Abis, L.; Dalcanale, E.; Du vosel, A.; Spera, S. Structurally new macrocycles from the resorcinol-aldehyde condensation. Configurational and conformational analyses by means of dynamic NMR, NOE, and T1 experiments, *J. Org. Chem.* **1988**, 53, 5475–5479.
- [30] (a) Botta, B.; Iacomacci, P.; Di Giovanni, M. C.; Delle Monache, G.; Gacs-Baitz, E. et al. The tetramerization of 2,4-dimethoxycinnamates. A novel route to calixarenes, *J. Org. Chem.* **1992**, 57, 3259–3261. (b) Botta, B.; Di Giovanni, M. C.; Delle Monache, G.; De Rosa, M. C.; Gacs-Baitz, E. et al. A novel route to calix[4]arenes. 2. Solution- and solid-state structural analyses and molecular modeling studies, *J. Org. Chem.* **1994**, 59, 1532–1541. (c) Botta, B.; Cassani, M.; D'Acquarica, I.; Misiti, D.; Subissati, D.; Delle Monache, G. Resorcarenes: emerging class of macrocyclic receptors, *Curr. Org. Chem.* **2005**, 9, 337–355.
- [31] Perrin, M.; Oehler, D. in *Calixarenes: A Versatile Class of Macrocyclic Compounds* (J. Vicens and V. Böhmer Eds., Kluwer Academic Publishers, Dordrecht, The Netherlands) **1991**; pp. 65–85.
- [32] D'Acquarica, I.; Nevola, L.; Delle Monache, G.; Gács-Baitz, E.; Massera, C. et al. Cyanoresorc[5]arenes: isolation; conformation and crystal structure, *Eur. J. Org. Chem.* **2006**, 16, 3652–3660.
- [33] Botta, B.; D'Acquarica, I.; Delle Monache, G.; Nevola, L.; Tullo, D. et al. Nitrosonium complexes of resorc[4]arenes: spectral, kinetic, and theoretical studies, *J. Am. Chem. Soc.* **2007**, 129, 11202–11212.
- [34] Ghirga, F.; D'Acquarica, I.; Delle Monache, G.; Toscano, S.; Mannina, L. et al. Undecenyl resorc[4]arene in the chair conformation as preorganized synthon for olefin metathesis, *RSC Adv.* **2013**, 3, 17567–17576.

- 1  
2  
3 [35] Cavallo, G.; Metrangolo, P.; Milani, R.; Pilati, T.; Priimagi, A. et al. The halogen bond, *Chem. Rev.*  
4 **2016**, 116, 2478–2601.  
5  
6 [36] Beyeh, N. K.; Pan, F.; Rissanen, K. A. Halogen-bonded dimeric resorcinarene capsule, *Angew.*  
7 *Chem. Int. Ed.* **2015**, 127, 7411–7415.  
8  
9 [37] Beyeh, N. K.; Cetina, M.; Rissanen, K. A. Halogen bonded analogues of deep cavity cavitands,  
10 *Chem. Commun.* **2014**, 50, 1959–1961.  
11  
12 [38] Dumele, O.; Trapp, N.; Diederich, F. Halogen bonding molecular capsules, *Angew. Chem. Int. Ed.*  
13 **2015**, 54, 12339–12344.  
14  
15 [39] Sarwar, M. G.; Ajami, D.; Theodorakopoulos, G.; Petsalakis, I. D.; Rebek, J. Amplified halogen  
16 bonding in a small space, *J. Am. Chem. Soc.* **2013**, 135, 13672–13675.  
17  
18 [40] El-Sheshtawy, H. S.; Bassil, B. S.; Assaf, K. I.; Kortz, U.; Nau, W.M. Halogen bonding inside a  
19 molecular container, *J. Am. Chem. Soc.* **2012**, 134, 19935–19941.  
20  
21 [41] Layne, J. Characterization and comparison of the chromatographic performance of conventional,  
22 polar-embedded, and polar-endcapped reversed-phase liquid chromatography stationary phases, *J.*  
23 *Chromatogr. A* **2002**, 957, 149–164.  
24  
25 [42] Simoni, D.; Romagnoli, R.; Baruchello, R.; Rondanin, R.; Rizzi, M. et al. Novel combretastatin  
26 analogues endowed with antitumor activity, *J. Med. Chem.* **2006**, 49, 3143–3152.  
27  
28 [43] Simoni, D.; Romagnoli, R.; Baruchello, R.; Rondanin, R.; Grisolia, G. et al. Novel A-ring and B-ring  
29 modified combretastatin A-4 (CA-4) analogues endowed with interesting cytotoxic activity, *J. Med.*  
30 *Chem.* **2008**, 51, 6211–6215.  
31  
32 [44] Pettit, G. R.; Singh, S. B. Isolation, structure, and synthesis of combretastatin A-2, A-3, and B-2,  
33 *Can. J. Chem.* **1987**, 65, 2390–2396.  
34  
35 [45] Aprile, S.; Del Grosso, E.; Tron, G. C.; Grosa, G. In vitro metabolism study of combretastatin A-4 in  
36 rat and human liver microsomes, *Drug Metab. Dispos.* **2007**, 35, 2252–2261.  
37  
38 [46] Pietrogrande, M. C.; Dondi, F.; Ciogli, A.; Gasparrini, F.; Piccin, A.; Serafini, M.; Characterization of  
39 new types of stationary phases for fast and ultra-fast liquid chromatography by signal processing  
40 based on AutoCovariance Function: a case study of application to *Passiflora incarnata* L. extract  
41 separations, *J. Chromatogr. A* **2010**, 1217, 4355–4364.  
42  
43 [47] Moni, L.; Ciogli, A.; D'Acquarica, I.; Dondoni, A.; Gasparrini, F.; Marra, A. Synthesis of sugar-based  
44 silica gels by copper-catalysed azide-alkyne cycloaddition via a single-step azido-activated silica  
45  
46  
47  
48  
49  
50  
51  
52  
53  
54  
55  
56  
57  
58  
59  
60

1  
2  
3 intermediate and the use of the gels in hydrophilic interaction chromatography, *Chem. Eur. J.* **2010**,  
4 16, 5712–5722.

5  
6 [48] Ghirga, F.; Quaglio, D.; Iovine, V.; Botta, B.; Pierini, M. et al. Synthesis of a double-spanned  
7 resorc[4]arene via ring-closing metathesis and calculation of aggregation propensity, *J. Org. Chem.*  
8 **2014**, 79, 11051–11060.

9  
10 [49] D'Acquarica, I.; Gasparrini, F.; Giannoli, B.; Badaloni, E.; Galletti, B. et al. Enantio- and chemo-  
11 selective HPLC separations by chiral-achiral tandem-columns approach: the combination of  
12 CHIROBIOTIC TAG™ and SCX columns for the analysis of propionyl carnitine and related impurities, *J.*  
13 *Chromatogr. A* **2004**, 1061, 167–173.

14  
15 [50] Gasparrini, F.; Cancelliere, G.; Ciogli, A.; D'Acquarica, I.; Misiti, D.; Villani, C. New chiral and  
16 restricted-access materials containing glycopeptides as selectors for the high-performance liquid  
17 chromatographic determination of chiral drugs in biological matrices, *J. Chromatogr. A* **2008**, 1191,  
18 205–213.

19  
20 [51] Kotoni, D.; D'Acquarica, I.; Ciogli, A.; Villani, C.; Capitani, D.; Gasparrini, F. Design and evaluation  
21 of hydrolytically stable bidentate urea-type stationary phases for hydrophilic interaction  
22 chromatography, *J. Chromatogr. A* **2012**, 1232, 196–211.  
23  
24  
25  
26  
27  
28  
29  
30  
31  
32  
33  
34  
35  
36  
37  
38  
39  
40  
41  
42  
43  
44  
45  
46  
47  
48  
49  
50  
51  
52  
53  
54  
55  
56  
57  
58  
59  
60